JOURNAL OF GEOPHYSICAL RESEARCH, VOL. 112, D11110, doi:10.1029/2006JD008054, 2007



# Changes in the variability of North Pacific Oscillation around 1975/1976 and its relationship with East Asian winter climate

Lin Wang,[1,2] Wen Chen,[1] and Ronghui Huang[1]

Received 19 September 2006; revised 15 February 2007; accepted 2 March 2007; published 7 June 2007.

[1] The variability of North Pacific Oscillation (NPO) and the associated atmospheric circulation in the boreal winter are studied with the HadSLP2, the National Centers for Environmental Prediction/National Center for Atmospheric Research (NCEP/NCAR), and the ECMWF 40-year reanalysis (ERA-40) data. The results show that the variability of NPO is not stationary with a typical period around 3 years during 1957–1975 and shifting to around 5–6 years after that. Linear correlation and regression analysis indicates that in the winters before 1975 the geopotential height field related to the NPO is characterized by a barotropic north-south dipole around the Pacific sector, which is the traditional NPO mode. In this subperiod, the El Niño/Southern Oscillation (ENSO) has a dominant influence on the NPO. There is anomalous stationary wave propagation associated with the NPO from the subtropical-central Pacific to the northern Pacific. And the NPO has no significant relations to the East Asian climate. In the winters after 1975, however, the atmospheric circulation related to the NPO exhibits a circum-global wave train pattern over the extratropical regions in the Northern Hemisphere. Particularly, the northward wave activity propagation is enhanced over the extratropics of East Asia. The remote forcing from the tropical eastern Pacific sea surface temperature anomalies becomes small. Hence the NPO has a close relationship with the circulation over East Asia during this period.

**Citation:** Wang, L., W. Chen, and R. Huang (2007), Changes in the variability of North Pacific Oscillation around 1975/1976 and its relationship with East Asian winter climate, *J. Geophys. Res.*, *112*, D11110, doi:10.1029/2006JD008054.

## 1. Introduction

[2] The North Pacific Oscillation (NPO), as first described by *Walker and Bliss* [1932], is a north-south seesaw of sea level pressure (SLP), involving one belt in high latitudes extending from eastern Siberia to western Canada and a broad region at lower latitudes including the subtropics and extending poleward to ~40°N. In the 1930s, the evidence in favor of the NPO was not convincing because of the sparsity of available data and the marginal level of many of the correlations. By using longer and more reliable data sets, *Kutzbach* [1970] and *Rogers* [1979] confirmed the existence of NPO in January and mean winter by eigenvector analysis, respectively. They showed that the second eigenvector of SLP field exhibited the NPO mode. *Wallace and Gutzler* [1981] reconfirmed the NPO by using the one-point correlation method for 45 winter months. *Rogers* [1981] described in detail the circulation and climatic variables related to the NPO, and claimed that the NPO resulted primarily from the shifts in the mean position of the Aleutian Low. Since then, there have been few literatures documenting the NPO because of its weak influence on the climate over North America and Europe.

[3] In contrast, the North Atlantic Oscillation (NAO) attracted more interest over recent decades because of its significant impacts on the Eurasian weather and climate [e.g., *van Loon and Rogers*, 1978; *Rogers and van Loon*, 1979; *Hurrell*, 1995, 1996; *Hurrell and van Loon*, 1997; *Hurrell et al.*, 2003]. The two oscillations have been shown to represent separate patterns of teleconnections of SLP [*Rogers*, 1981; *Wallace and Gutzler*, 1981]. The NAO is the dominant mode of variability in the North Atlantic region and shows variability on all timescales. Many studies suggest that the interannual to quasi-decadal sea surface temperature (SST) variation in the North Atlantic is strongly correlated to the atmospheric circulation over that area [e.g., *Bjerknes*, 1964; *Deser and Blackmon*, 1993; *Kushnir*, 1994]. However, a recent work by *Walter and Graf* [2002] found that the correlation between the NAO and the North Atlantic SST is not stationary, and that it depends on the variability of the NAO index. When the NAO index is characterized by a pronounced decadal variability and by mainly positive values, the North Atlantic SST is strongly correlated to the regional atmospheric circulation in the North Atlantic sector: NAO. On the contrary, remote influence, in particular from the tropical Pacific region, becomes important when the NAO index is characterized by weak decadal variability.

[1] Center for Monsoon System Research, Institute of Atmospheric Physics, Chinese Academy of Sciences, Beijing, China.
[2] Graduate University of Chinese Academy of Sciences, Beijing, China.


0148-0227/07/2006JD008054$09.00

[4] In the North Pacific area, the NPO is the most important teleconnection mode. The atmosphere-ocean interaction is also strong and important over this area [*Wallace and Jiang*, 1987; *Wallace et al.*, 1990]. It is generally recognized that the NPO influences the climate over the "downstream" region of North America [*Rogers*, 1981], rather than on the climate over the "upstream" regions such as East Asia. However, more recent studies present a close relation between NPO and the East Asian Winter Monsoon (EAWM) [*Guo and Sun*, 2004]. They found that the EAWM becomes weaker when the NPO is strong, with an extensive high temperature in China, less rainfall in the middle-lower reaches of the Yangtze River, and more rainfall in South China. Hence we need to explore if there is a change in the influences of the NPO, and particularly to know why this has happened. We will show that there are clear changes in the variability of NPO, and the associated circulation patterns and SST anomalies. The data sets used in our study are described in section 2. The NPO index is derived and its characteristics are presented in section 3. Section 4 then presents the changes of NPO-associated circulation patterns and its relationship with the wintertime East Asian climate. In section 5, we discuss why there is such a change in the pattern of NPO. Finally, a summary is presented in section 6.

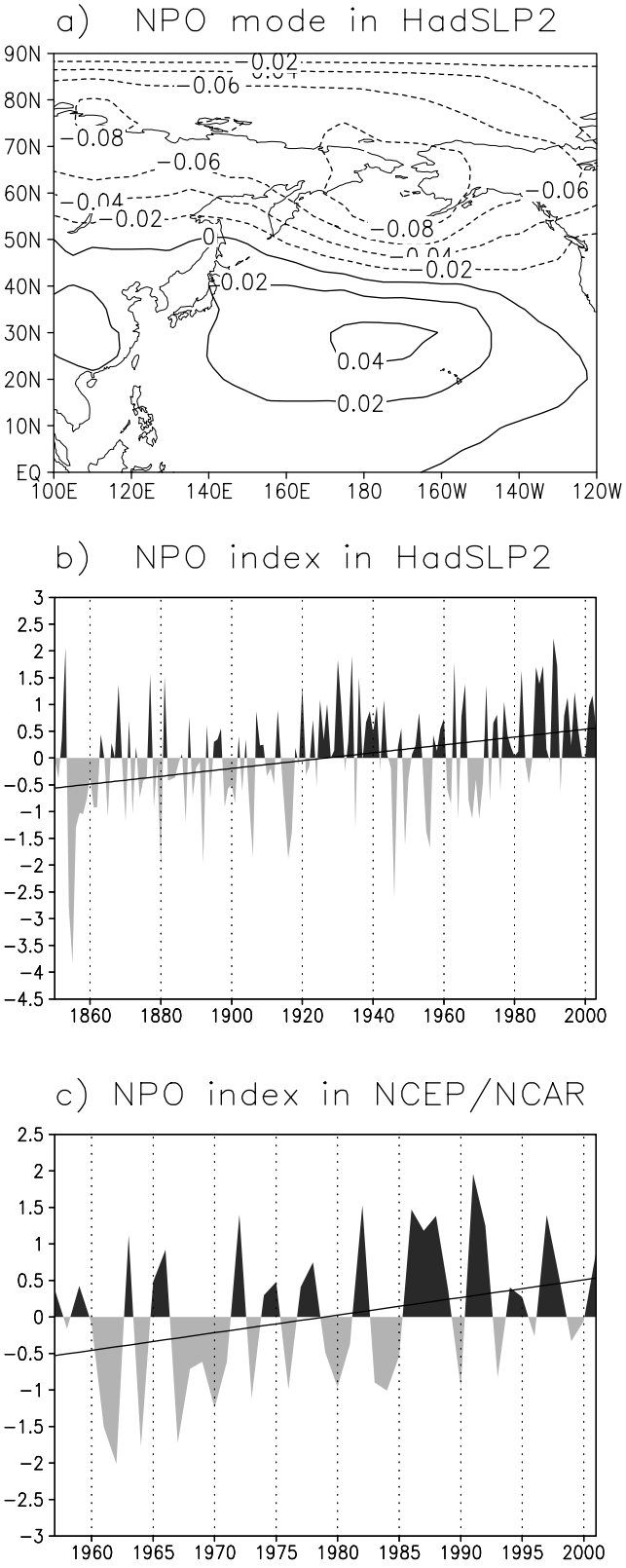


## 2. Data Description

[5] Atmospheric data used in this study include the reanalysis data set from the National Centers for Environmental Prediction/National Center for Atmospheric Research (NCEP/NCAR [*Kalnay et al.*, 1996; *Kistler et al.*, 2001]), covering the years from 1948 to present. This data set has a 2.5° × 2.5° horizontal resolution and extends from 1000 to 10 hPa with 17 vertical pressure levels. Atmospheric data also include the ERA-40 reanalysis from the European Center for Medium-Range Weather Forecasts (ECMWF), which covers 45 years from September 1957 to August 2002 [*Uppala et al.*, 2005]. This data set has the same horizontal resolution as the NCEP/NCAR one and extends from 1000 to 1 hPa with 23 vertical pressure levels. The ERA-40 reanalysis data are used to validate the results derived from NCEP/NCAR reanalysis. For the NCEP/NCAR reanalysis, we only adopt those from 1957 to 2002 in order to avoid the relatively unreliable data before 1957. We also employ the Met Office Hadley Center's mean sea level pressure data set, HadSLP2, which is a unique combination of monthly globally complete fields of land and marine pressure observations on a 5° × 5° grid from 1850 to 2004 [*Allan and Ansell*, 2006]. This data set has proved to be particularly valuable as a means of generating indices and spatial fields over the North Pacific, especially those related to the Aleutian Low [*Allan and Ansell*, 2006].

[6] Oceanic data used in this study are the Met Office Hadley Center's sea ice and sea surface temperature data set (HadISST1). It is a unique combination of monthly globally

**Figure 1.** (a) The second EOF mode of the winter mean SLP field for the years 1850–2003 using HadSLP2. (b) The corresponding normalized principal component (PC) time series for the mode in Figure 1a. (c) The normalized PC2 time series of the winter mean SLP field for the years 1957–2001 using NCEP/NCAR reanalysis. Dark (light) shade in Figures 1b and 1c indicates positive (negative) value of NPO index.

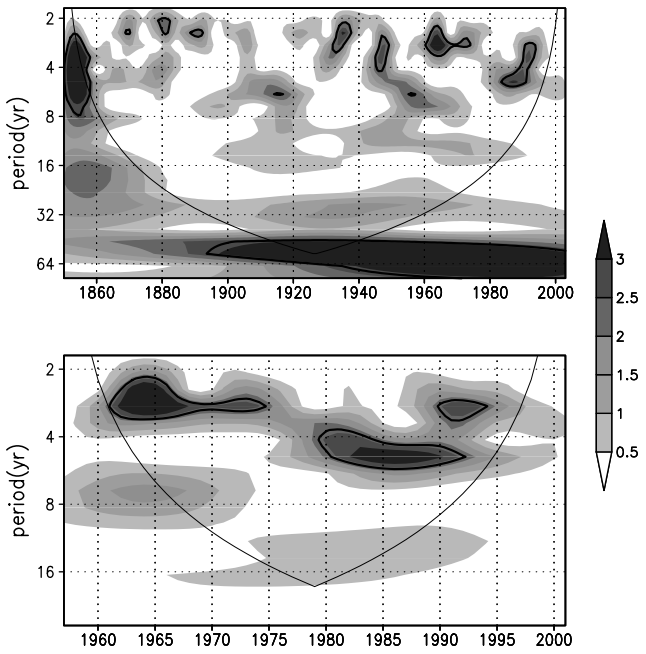


**Figure 2.** Local wavelet power spectrum of the winter mean normalized NPO index for the years (a) 1850–2003 using HadSLP2 data, and (b) 1957–2001 using NCEP/NCAR reanalysis. The black contour is the 90% significance level using a white noise background spectrum.

complete fields of SST and sea ice concentration on a 1° latitude-longitude grid from 1870 to date [*Rayner et al.*, 2003].

[7] In this study, we focus on the wintertime large-scale interannual variability near or at the surface and in the troposphere. Every analysis is performed with raw instead of detrended data. Seasonal data are used throughout this study and they are constructed by averaging December, January, and February (DJF) resulting in 45 winter fields.

## 3. The NPO Index and the Change in its Variability

[8] The North Pacific Oscillation was first described by *Walker and Bliss* [1932] as the opposite pressure variation over Hawaii and over Alaska and Alberta. Similar SLP patterns were suggested by eigenvector analyses of mean January [*Kutzbach*, 1970] and mean winter [*Rogers*, 1979] SLP anomaly data. It was also obvious in the one-point correlation map of SLP field for winter months [*Wallace and Gutzler*, 1981]. In this study, we adopted the EOF analysis on the winter mean SLP anomaly field to obtain the NPO mode and the corresponding index. The area we chose extends from 100°E to 240°W and from 0° to 90°N. When performing EOF analysis, the data field was properly weighted to account for the decrease of area toward the Pole [*North et al.*, 1982a].

[9] The leading EOF of SLP anomaly field derived from 1850 to 2003 using HadSLP2, which explains 38.3% of the total variance, depicts variability in the intensity of the Aleutian low in winter. *Trenberth and Hurrell* [1994] defined a north Pacific (NP) index as the area-weighted mean SLP over the north Pacific, which also measures the changes in the intensity of the Aleutian low. In fact, the correlation of the time series of EOF1 with the NP index for DJF averages is 0.95 for 1850–2003, which is far above the 99% statistical significance. Hence the climate variations over the north Pacific associated with the EOF1 of SLP have been documented by a number of studies. The second eigenvector of SLP anomaly field, which explains 22.2% of the total variance, exhibits a north-south dipole in the Pacific sector with one center around 60°N, 170°W, and the other around 30°N, 180°W as shown in Figure 1a. It resembles the traditional NPO pattern described by *Wallace*

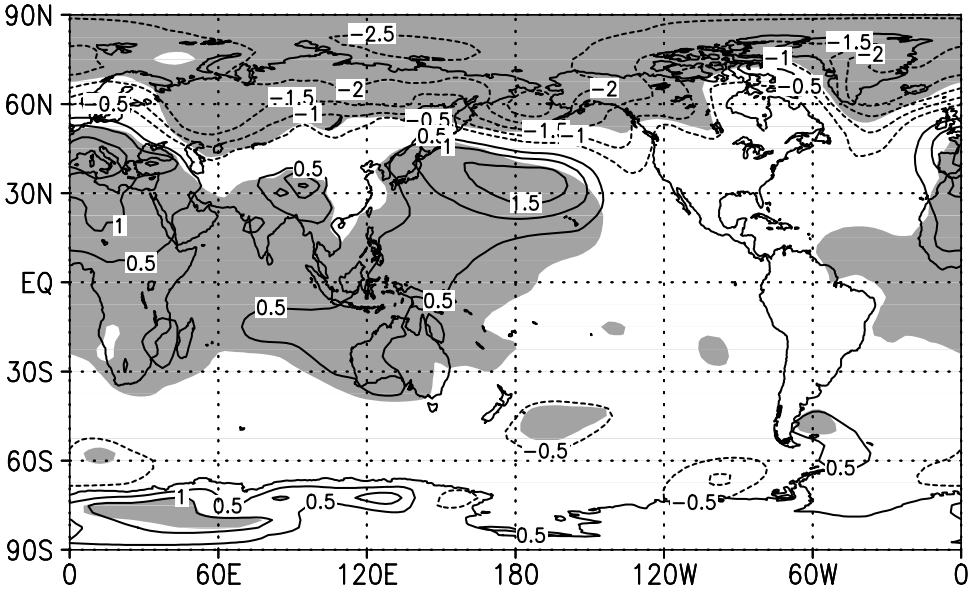


**Figure 3.** Regression (contours)/correlation (shading) maps for the SLP field on the normalized NPO index based on the winter data from 1957 to 2001 using NCEP/NCAR reanalysis. The shading indicates that the correlation is significant above the 95% level. Contour interval is 0.5 hPa.

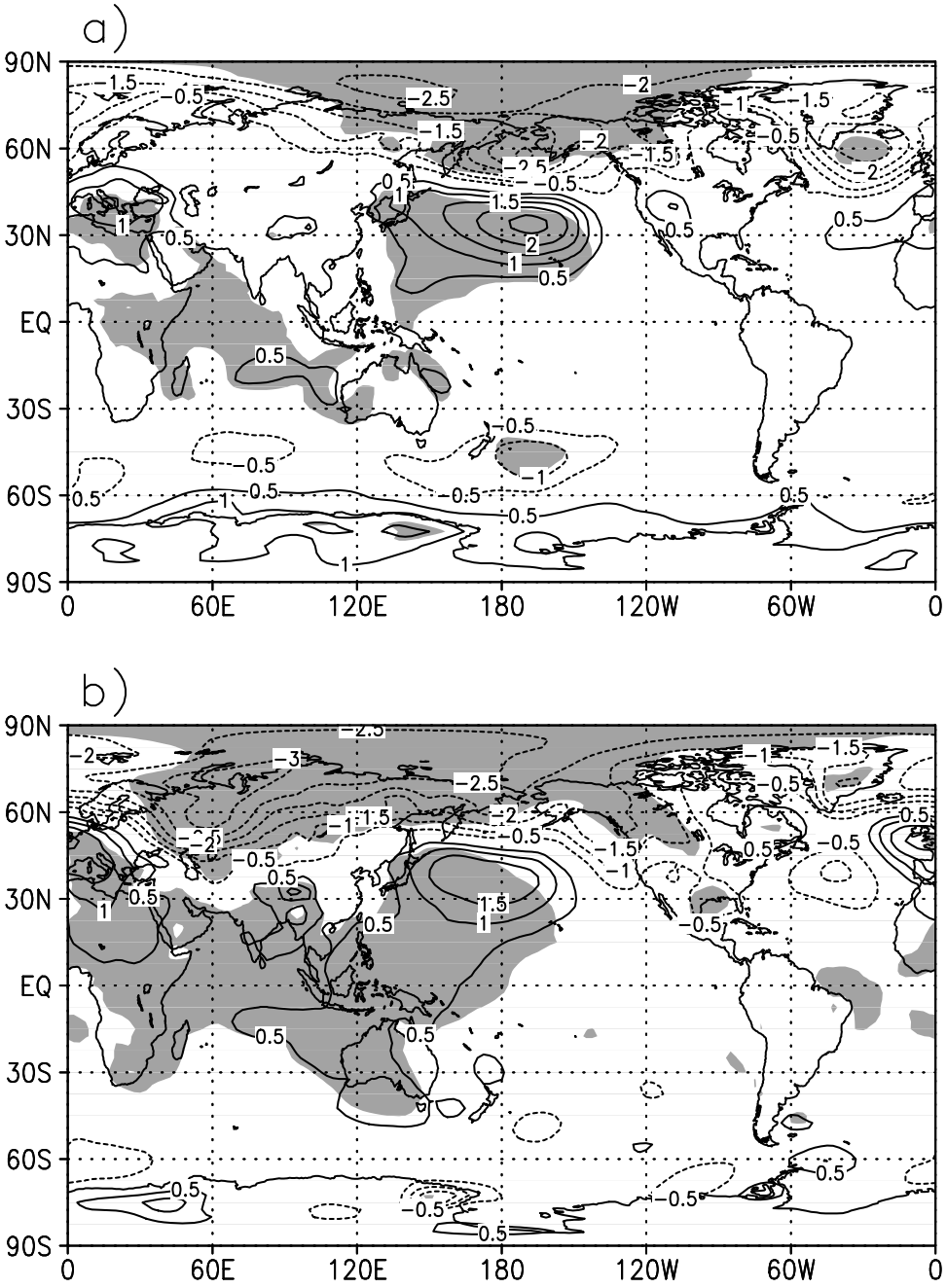


**Figure 4.** Regression (contours)/correlation (shading) maps for the SLP field on the normalized NPO index based on the winter data for (a) regional period (1957–1975) and (b) global period (1976–2001) using NCEP/NCAR reanalysis. The shading indicates that the correlation is significant above the 95% level. Contour interval is 0.5 hPa.

*and Gutzler* [1981] although here the centers of action are about 20° east. Applying the guidelines by *North et al.* [1982b], we find that both first and second EOFs are adequately separated from the remaining modes. The corresponding time series (Figure 1b) of EOF2 are defined as the NPO index, which has clear linear trend toward its positive polarity with statistical significance above 99%. The convention here is that the "1850" winter is actually 1850/1851 and so on. The variability of this index has not been uniform since the beginning of the data. We applied a Morlet wavelet analysis [*Torrence and Compo*, 1998] to the winter mean NPO index. The local wavelet power spectrum is presented in Figure 2a. Our null hypothesis states that the NPO index is a nearly white autoregressive (AR-1) noise time series with autocorrelation coefficient 0.08. The significance of the local wavelet power spectrum was therefore tested using a white noise background spectrum. Figure 2a shows several peaks of wavelet power for periods between 2 and 70 years. Especially, fluctuations with periods around 3 years are pronounced from 1960 to 1975. From 1980

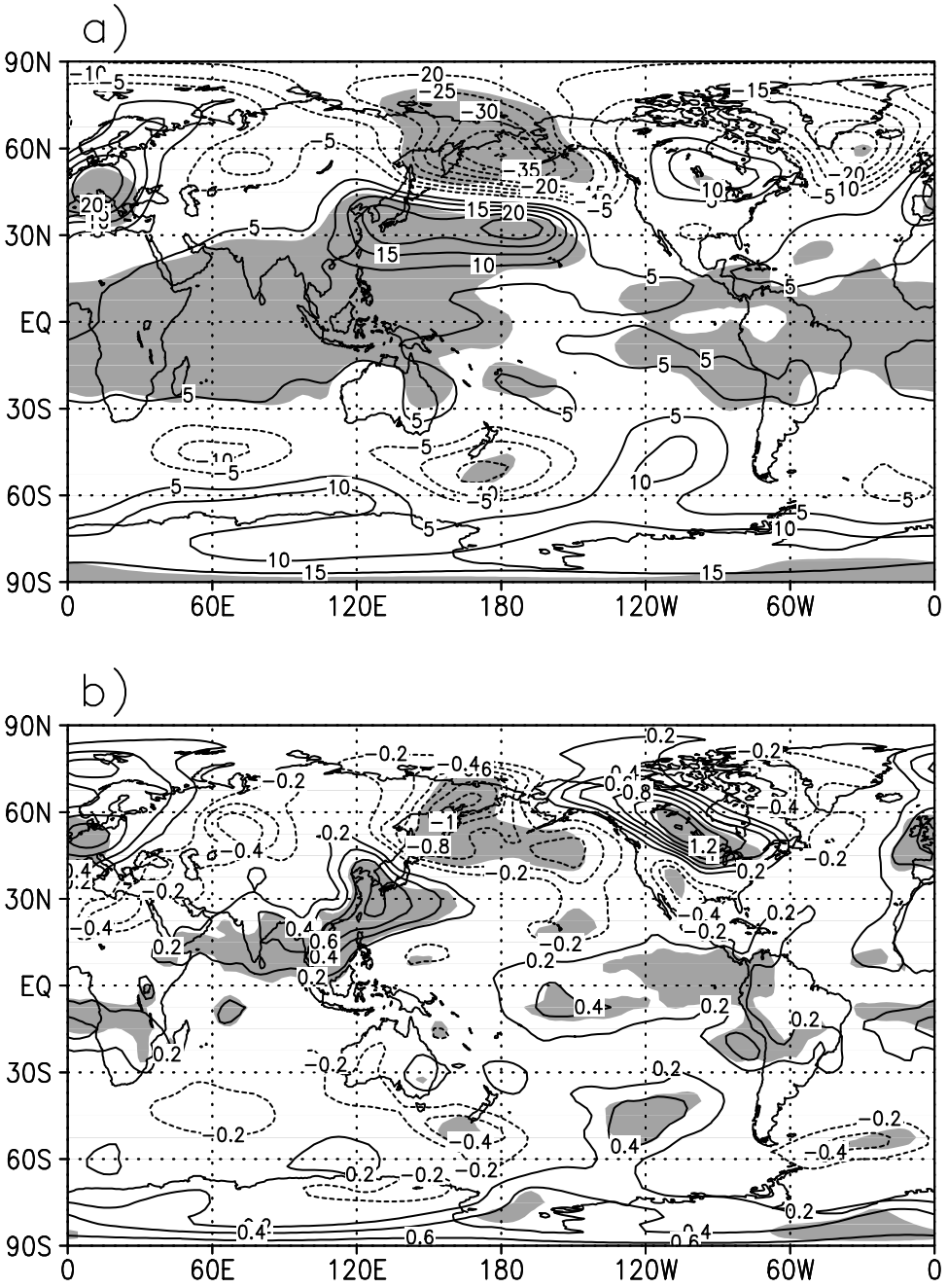


**Figure 5.** Regression (contours)/correlation (shading) maps for (a) the geopotential height at 500 hPa and (b) the air temperature at 850 hPa on the normalized NPO index based on the winter data for regional period (1957–1975) using NCEP/NCAR reanalysis. The shading indicates that the correlation is significant above the 95% level. Contour intervals are 5 m in Figure 5a and 0.2°C in Figure 5b.

onward, there is another peak for periods between 3 and 7 years. These peaks are significant above the 90% level. Generally, the NPO shows pronounced interannual variability with interdecadal changes in the available data time.

[10] We further calculated the NPO index from 1957 to 2001 using the NCEP/NCAR SLP (Figure 1c). It is well correlated to the NPO index derived from HadSLP2 data set during the same period, with the correlation coefficient 0.94 above 99% confidence level. The local wavelet power spectrum (Figure 2b) resembles the results from HadSLP2 for the time period 1957–2001, too. A clear shift in the variability of the NPO appears around 1975/76. Hence in the following of this paper, two subperiods will be discussed separately in order to take into account this change. One subperiod ranges from 1957 to 1975, characterized by a pronounced 3-year variability of NPO index. The other period ranges from 1976 to 2001, characterized by pronounced 5–6 years variability. Although the index has a significant linear trend, the results derived from detrended data are very similar to those based on raw data. Thus only

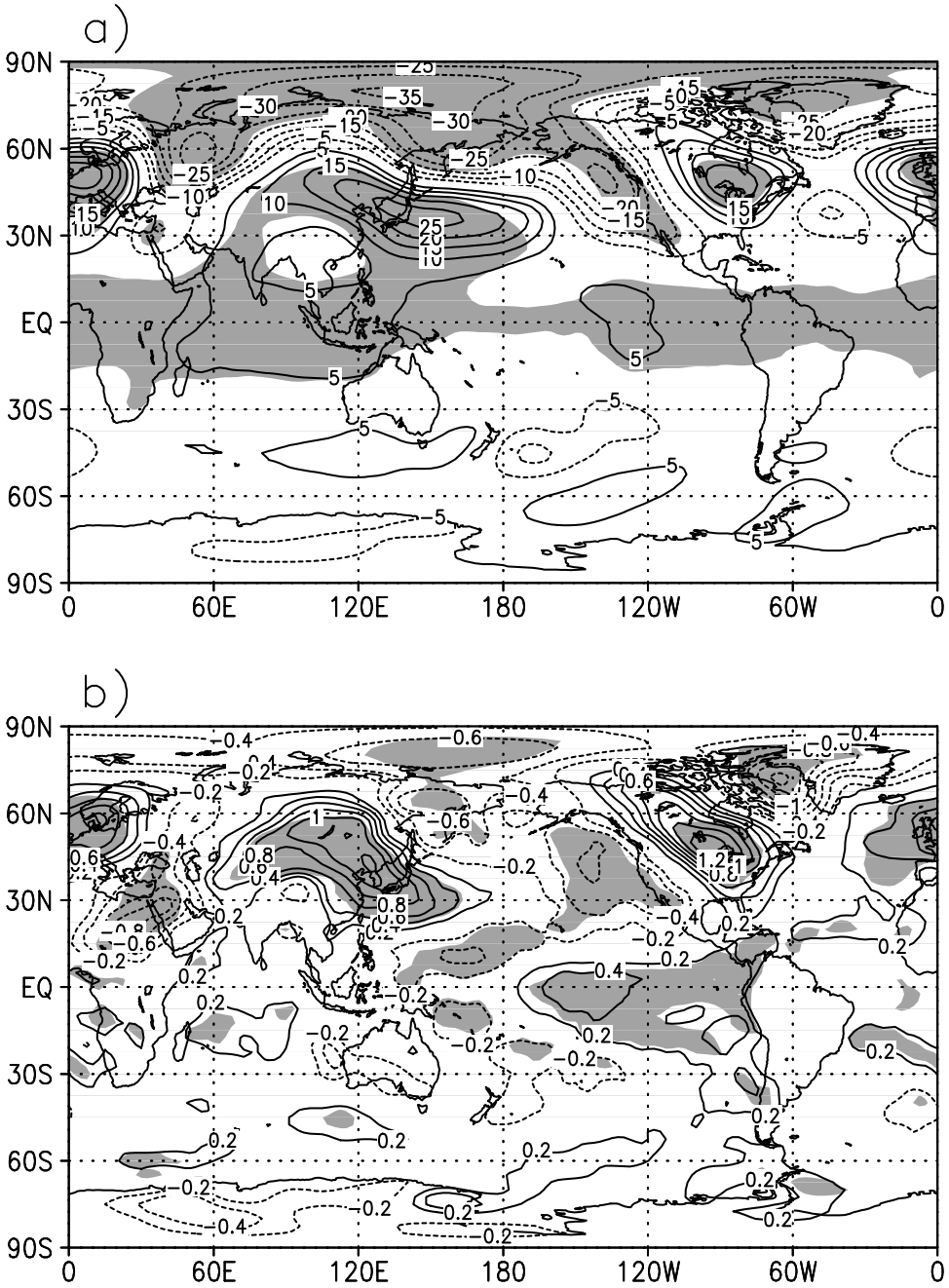


**Figure 6.** The same as in Figure 5, but for the global period (1976–2001).

the results by use of the raw data are presented in this paper.

## 4. Changes in the Associated General Circulation Patterns

[11] As mentioned in section 1, the North Pacific Oscillation exhibits a north-south seesaw of sea level pressure in the Pacific area, which can be clearly seen in the regression and correlation map of SLP on the winter mean NPO index for the period 1957–2001 (Figure 3). The correlation in the Pacific area is significant above 95% confidence level. Significant negative correlations extend zonally to cover the area from midlatitudes to polar region, and positive signals extend to Indian Ocean and African continent. However, when we divide the period into two subperiods 1957–1975 and 1976–2001 according to the shift in the variability of NPO, big differences emerge in the regression map of SLP on the NPO index. During the first subperiod (1957–1975, Figure 4a), the NPO is strongly correlated to the local SLP with larger regression coefficients in the North Pacific. In contrast, during the second subperiod 1976–2001, instead of one "center of action" near Bering Strait, a belt of high correlation coefficients appears in the north of 50°N from Europe to North America as shown in Figure 4b. Meanwhile, the opposite correlations at lower latitudes expand to Indian Ocean and African continent. In addition, the regressed centers of action can be discerned to

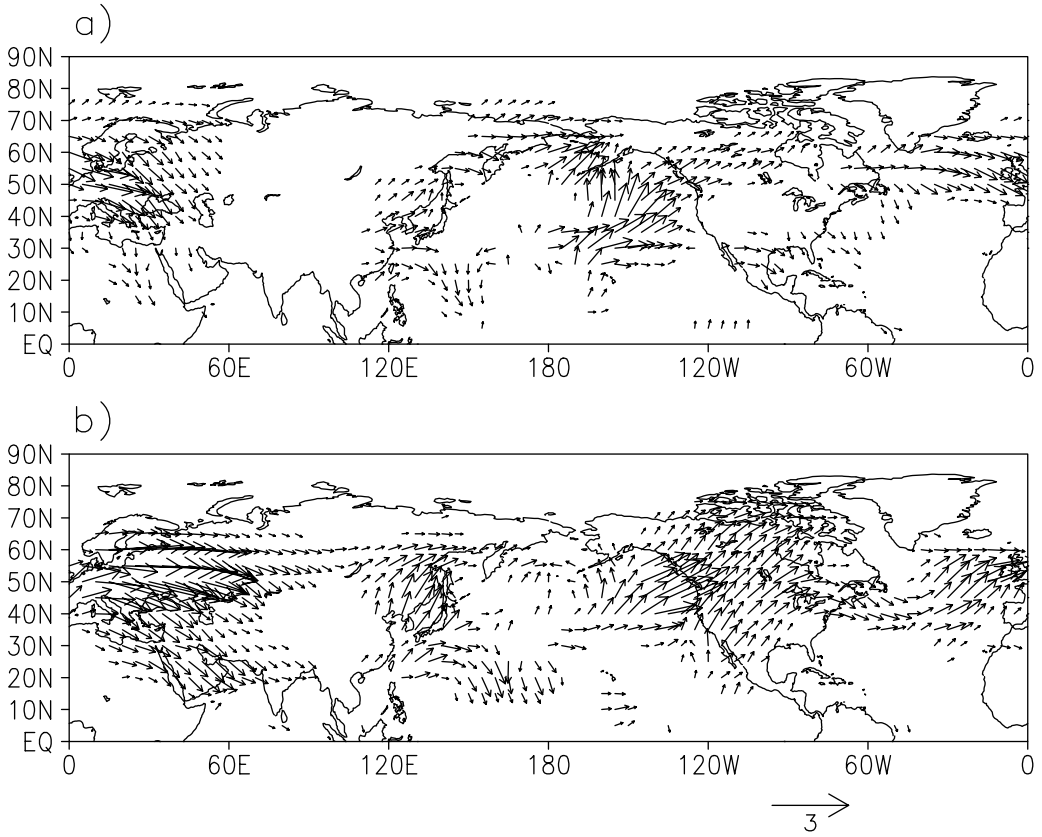


**Figure 7.** The horizontal stationary wave activity flux (in $m^2\ s^{-2}$) at 500 hPa associated with the NPO pattern based on the winter data for total wave numbers in (a) regional period and (b) global period, with scale shown bottom right.

be shifted from the east to the west of the dateline. Hence we shall refer to the former period 1957–1975 as the "regional period" and to the latter period 1976–2001 as the "global period" in the rest part of this paper.

### 4.1. Regional Period

[12] Figure 5a shows the linear regression coefficients between the NPO index and the 500 hPa geopotential height, which mainly display a dipole pattern with negative height anomaly centered west of Bering Strait and positive one at 30°N centered east of the dateline. This dipole structure resembles the classical meridional seesaw pattern associated with the North Pacific Oscillation [e.g., *Wallace and Gutzler*, 1981], and the correlations in both centers of the dipole are significant above the 95% level. We also found that this dipole in the geopotential height map has a pronounced barotropic structure extending from lower level of troposphere to the tropopause region (figures not shown).

[13] As mentioned in section 1, recent studies found that the NPO is closely related to the East Asia Winter Monsoon. The temperature and the intensity of Siberian High (SH) are often used to indicate the variability of EAWM [e.g., *Gong et al.*, 2001]. Hence we present the low-level (850 hPa) temperature anomalies related to the NPO to see whether the relation between NPO and the air temperature over East Asia is different in the two subperiods. In the regional period (Figure 5b), positive temperature anomalies are mainly located to the south and southeast of Eurasian continent, including the East China Sea, the South China Sea, the maritime continent, and the north Indian Ocean. The negative anomalies locate in the North Pacific around 60°N, which is consistent with previous results [e.g., *Rogers*, 1981]. Obviously, the signals over East Asia are weak in the inner continent and only significant along and off the coasts. The correlation coefficient between NPO index and SH index, which is defined after *Gong et al.* [2001], is 0.00. This result implies that the NPO has no relation with the circulation at higher latitudes over East Asia in this subperiod.

### 4.2. Global Period

[14] During the time from 1976 to 2001, significant signals appear to the upstream of North Pacific as shown in Figure 4b. This feature can be more clearly seen in the regressed 500 hPa geopotential height field on the NPO index (Figure 6a), where wave train-like patterns emerge in the extratropical regions of Northern Hemisphere. The positive anomalies lie over the West Europe, the east of North America, and large areas from mid-Asia across Japan to North Pacific. The negative anomalies occupy the Ural region, the northern part of Greenland, and large areas from east Siberia to the northwest of North America. This wave train-like structure is quite different from the classical NPO pattern and implies an upper reach relation to the NPO. The pattern in 500 hPa geopotential height field also has a pronounced barotropic structure extending from lower level of troposphere to the tropopause region (figures not shown).

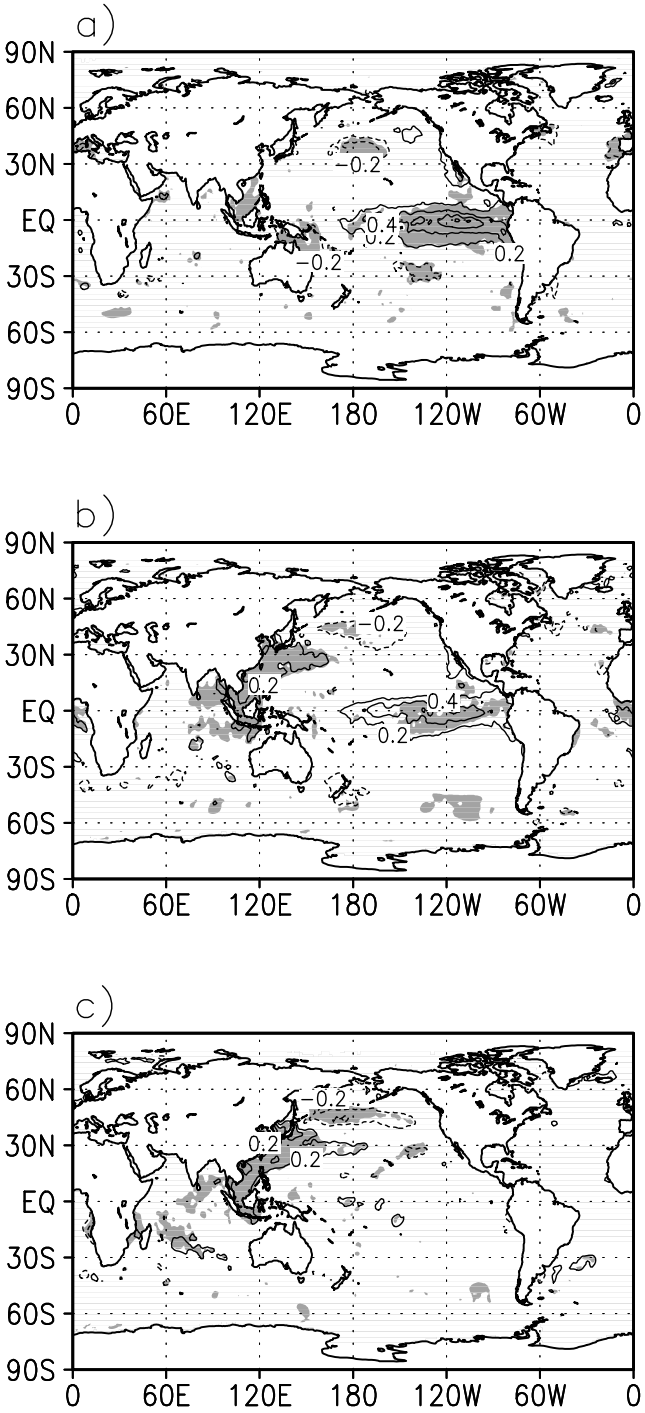


**Figure 8.** Regression (contours)/correlation (shading) coefficient for the SST field on the normalized NPO index based on the winter data for regional period (1957–1975). The SST is the seasonal mean of (a) the preceding autumn (SON), (b) the simultaneous winter (DJF), and (c) the following spring (MAM). The shading indicates that the correlation is significant above the 95% level.

[15] The 850-hPa air temperature anomalies associated with NPO is presented in Figure 6b for the global period. The biggest difference from that in regional period appears in Asia. From the east of the Caspian Sea, positive temperature anomalies extend northeastward to the Siberia and then southeastward to Japan, with central regressed value exceeding 1.2°C. From the Northeast Africa to Arabia, a negative temperature anomaly emerges. These signals are all significant above 95% confidence level. The pattern over the tropical Pacific and North America does not change much from the previous period to this period. Obviously, the temperature variations over East Asian continent are closely linked to the NPO. This result is consistent with the geopotential height changes associated with the NPO in the same period. Again, we calculate the correlation coefficient between the NPO and SH indices, and it shows −0.55 which is above 95% confidence level. Hence we can conclude that the NPO has a close relation with the circulation over East Asia in the global period.

## 5. Discussions

[16] In the previous section, two periods of time with different NPO variability have been studied separately. These periods were found to be characterized by different NPO-related circulation patterns, and particularly by different climatic anomalies over East Asia. The question is why there are changes in the pattern and influence of NPO.

[17] The wave activity in the atmosphere is important to understand the atmospheric motions and variability. Although the dynamical mechanism of NPO is still not clear, the significant wave train pattern in the global period (see Figure 6) evokes us to seek the relationship between the NPO and the atmospheric waves. As the Eliassen-Palm flux (EP flux, *Andrews et al.* [1987]; *Plumb* [1985]) is parallel to the group velocity of stationary waves, it is a good indicator for the propagation of stationary waves in the atmosphere. Therefore we calculated the wave activity flux for the anomalous stationary waves from the height anomalies which is the regression of the winter mean height against the NPO index. This way is similar to what *Karoly et al.* [1989] did for several cases including the Pacific-North America (PNA) patterns. Figure 7 shows the horizontal stationary wave activity flux at 500 hPa associated with the NPO pattern in the two subperiods. In general, there are anomalous propagations of wave activity in the hemispheric scale in both subperiods. The common feature in

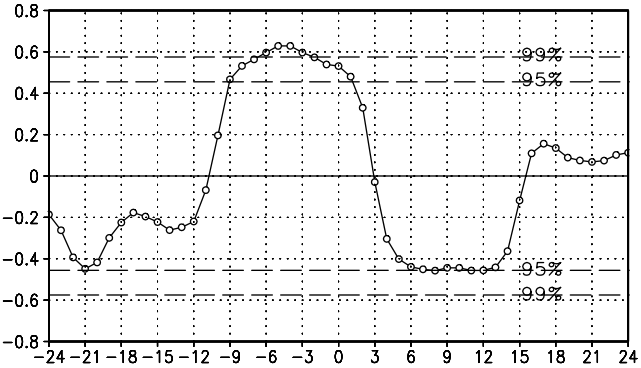


**Figure 9.** Lag-correlations between the NPO index and the Niño3 index for the regional period (1957–1975). The data are smoothed by 3-month running means.

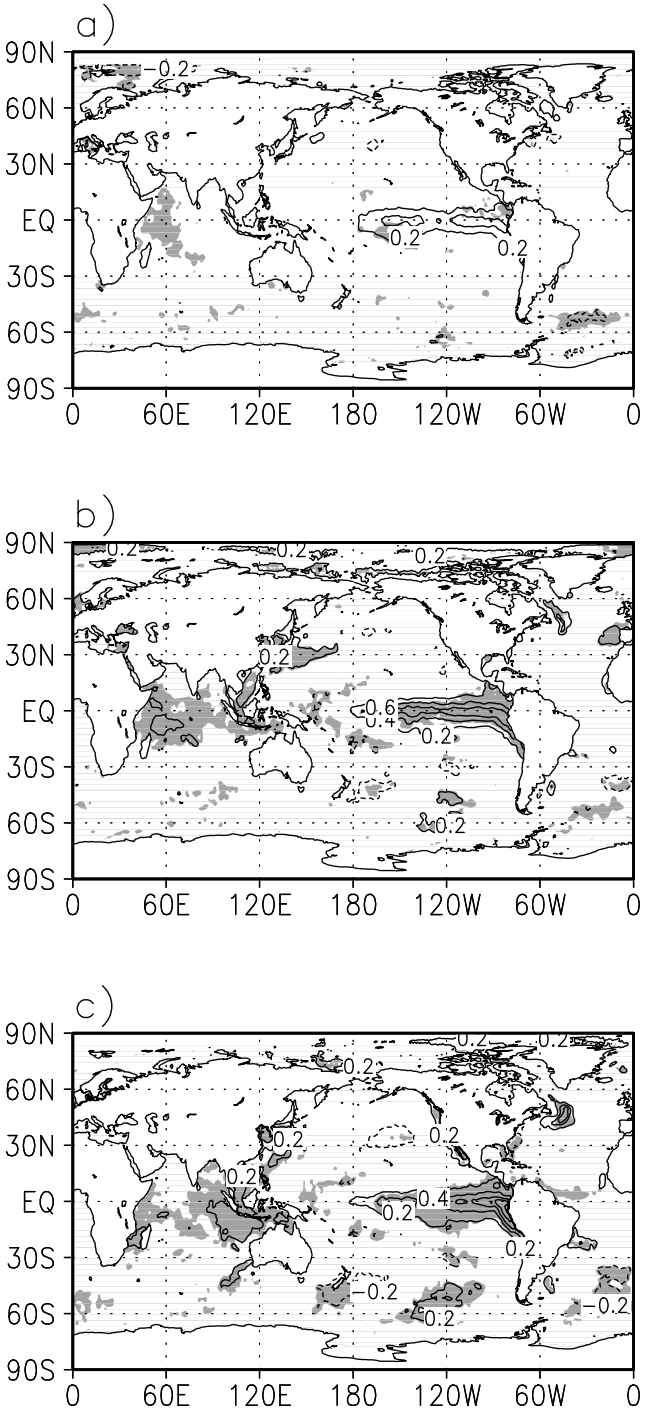


**Figure 10.** The same as in Figure 8, but for the global period (1976–2001).

Figures 7a and 7b is that the waves propagate eastward with three source regions in eastern Asia, the north Pacific, and the northern Atlantic, which resembles the climatology of DJF mean wave activity flux as shown in the work of *Yang and Gutowski* [1994]. However, the differences between these two periods are also obvious. In the regional period, anomalous wave activities are strong in the north Pacific, but are relatively weak in other regions (Figure 7a). Moreover, the source of wave activity in the north Pacific is located in the subtropical-central Pacific. This corresponds well to the elongated dipole mode of the NPO in Figure 5a. In the global period, the anomalous wave activities are still strong in the north Pacific, but the source of wave activity shifts to the subtropical-eastern Pacific (Figure 7b). And the PNA-like wave train appears much clearer than that in the regional period. In addition, there are much stronger wave activities in the Eurasian area than those during the regional period, which is consistent with the results in previous section. Hence the different circulation patterns associated with the NPO are suggested to be related to the anomalous stationary wave activities. In the regional period, there is anomalous stationary wave propagation from the subtropical-central Pacific to the northern Pacific. This wave activity corresponds to the elongated dipole structure of the NPO in the Pacific sector. However, in the global period, this northward propagation of wave activity shifts to the eastern Pacific. In the meantime, the northward wave propagation is enhanced over the extratropics of East Asia. Hence the center of NPO is shifted to the west of the dateline.

[18] The stationary planetary waves in the atmosphere are forced by orography and patterns of diabatic heating arising from the distribution of land and oceans [*Andrews et al.*, 1987]. The SST changes, which may induce diabatic heating anomaly, are also able to excite [*Horel and Wallace*, 1981] and modulate the variability of stationary waves [*Chen et al.*, 2003]. Here we will show the different roles played by anomalous SST for the two subperiods. Figure 8 presents the lead-lag regression and correlation maps of SST upon the DJF NPO index in the regional period as a check of the possible oceanic influence on the atmosphere. In the simultaneous correlation as shown in Figure 8b, a remarkable positive signal in SST field appears over the central and eastern tropical Pacific. This spatial structure can be easily identified to be in association with the El Niño/Southern Oscillation (ENSO). When there is a warm event, the NPO is in its positive phase, and the situation tends to be reversed for a cold event. These positive correlations in the tropical eastern Pacific are even stronger in the preceding autumn (Figure 8a). On the contrary, in the following spring, the signals over the tropical Pacific disappear (Figure 8c). This feature can also be clearly seen from the lag-correlations between the NPO index and the Niño3 index (Figure 9). The significant

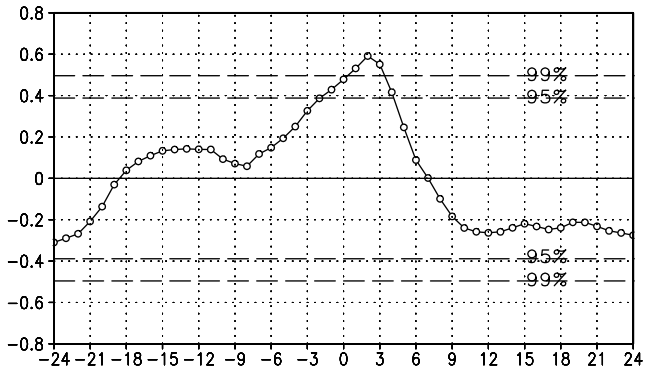


**Figure 11.** The same as in Figure 9, but for the global period (1976–2001).

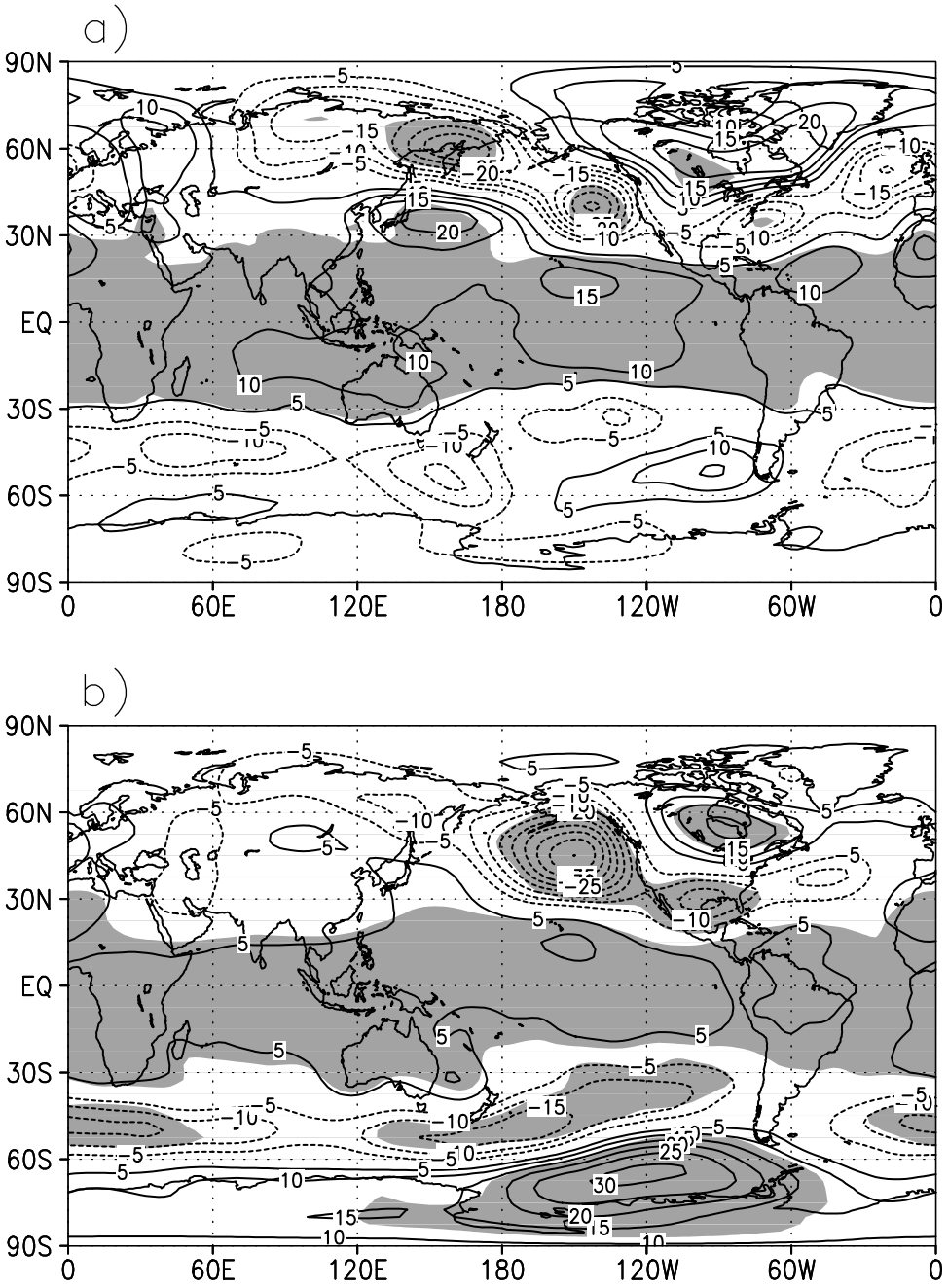


**Figure 12.** Regression (contours)/correlation (shading) maps for the 500-hPa geopotential height on the normalized Niño3 index based on the winter data for a) regional period (1957–1975) and b) global period (1976–2001) using NCEP/NCAR reanalysis. The shading indicates that the correlation is significant above the 95% level.

correlations start from the preceding spring and persist to the simultaneous winter with confidence level exceeding 95%. These results suggest a dominant influence of the tropical SST on the atmospheric circulation over North Pacific in the regional period. In the global period, although the simultaneous relationship of SST with the NPO index is similar in the tropical eastern Pacific to that in the regional period (Figure 10b), this signal cannot be traced back to the preceding season (Figure 10a) but last to the following spring (Figure 10c). This feature is also clear in the lag-correlations between the NPO index and the Niño3 index (Figure 11). Hence in the global period the ENSO is not the dominant factor to influence the NPO at all.

[19] To see how the atmosphere responds to the tropical eastern Pacific SST anomaly, we further calculated the regression map of 500 hPa geopotential height on the Niño3 index for the regional and the global period, respectively. In the regional period (Figure 12a), it is evident that anomalous SST in the tropical eastern Pacific may excite a PNA pattern, which is mainly confined to the northeast of the Pacific. To the northwest of the PNA wave train, a meridional dipole

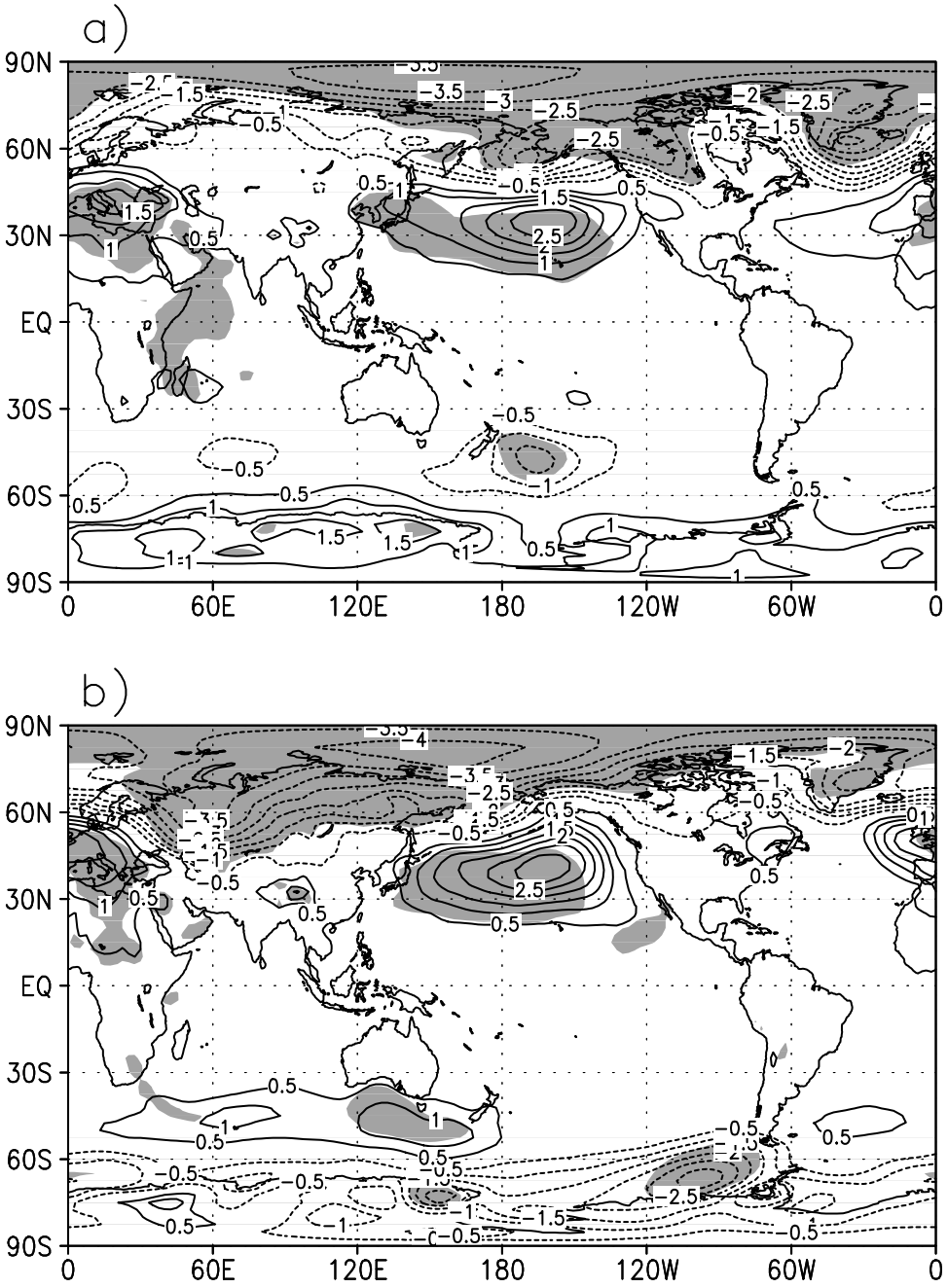


**Figure 13.** Regression (contours)/correlation (shading) maps for the SLP field on the normalized ENSO-removed-NPO index based on the winter data for (a) regional period (1957–1975) and (b) global period (1976–2001) using NCEP/NCAR reanalysis. The shading indicates that the correlation is significant above the 95% level.

emerges along the 160°E with one center at 60°N and the other at 35°N, which resembles the western Pacific pattern [*Wallace and Gutzler*, 1981]. Hence the influence of ENSO is superimposed on the NPO mode and makes the NPO like a slave. However, in the global period, the atmospheric response to the tropical SST anomalies is different from that in the regional period. The regression of 500h Pa geopotential height on the Niño3 index (Figure 12b) exhibits a very remarkable PNA pattern. However, the ENSO has no effect on the height over the western North Pacific. Therefore in this global period the NPO may link to other anomalies in the atmospheric circulation far beyond North Pacific.

[20] In order to see the effect of tropical eastern Pacific SST more clearly, the coherent variability of Niño3 index is removed by means of a linear regression from the time series of the NPO index as follows,

$$\mathrm{NPO}_{res} = \mathrm{NPO} - \mathrm{r} \times \mathrm{Ni\tilde{n}o3}$$

where NPO and Niño3 are normalized indices and $r$ is the correlation coefficient between them. After the ENSO signal

is removed, the NPO patterns in the two subperiods are more alike at both the surface (Figure 13) and the upper levels (figures not shown). Therefore it can be concluded that the forcing from eastern tropical Pacific SST plays a dominant role on the changes of NPO variability.

[21] It is already known that the NCEP/NCAR reanalysis data set is affected by two major changes in the observing system [*Kistler et al.*, 2001] and has been found to have a problem in the East Asian area around the middle of the 1970s [*Yang et al.*, 2002; *Wu et al.*, 2005]. Hence it is necessary to verify the above findings regarding the variability of NPO with other independent data set. We then adopted the ERA-40 data set from ECMWF to perform this confirmation. Comparisons of the results using the two different data sets present consistent features of the changes in variability of NPO around mid-1970s and its relationship with East Asian winter climate. Thus we may conclude that the results in this paper are robust and not data-dependent.

## 6. Summary

[22] The NPO mode and associated atmospheric circulation patterns in the boreal winter are analyzed by using the winter mean (DJF) data from the HadSLP2, the NCEP/NCAR and the ERA-40 reanalysis. The variability of NPO mode has been shown to be not uniform for the available data period. The Morlet wavelet analysis on the winter mean NPO index indicates that fluctuations with periods around 3 years are pronounced before 1975. However, the variability of 5- to 6-year periods is dominant after that. Hence the whole data set (1957–2001) is divided into two subperiods: the regional period (1957–1975) which is characterized by pronounced 3-year variability and the global period (1976–2001) when the 5- to 6-year variability is dominant. Linear correlation and regression analysis indicate that the atmospheric circulations associated with NPO are also different for these two subperiods. In the regional period, the geopotential height field related to the NPO is characterized by a barotropic north-south dipole in the Pacific sector with one center over west of Bering Strait and the other at 30°N extending from Korea peninsula to the dateline, which is similar to the traditional NPO mode described by previous studies [e.g. *Wallace and Gutzler*, 1981]. The correlation coefficient between the NPO and SH indices is very small, which imply that the NPO has no significant relationship with East Asian climate in this period. In the global period, however, the atmospheric circulation related to the NPO is quite different from that in the regional period and exhibits a circum-global wave train pattern over the extratropical regions in the Northern Hemisphere. In addition, the NPO has been shown to have a close relation with the circulation over East Asia in the global period.

[23] The reasons for the changes in NPO pattern and its influence are suggested to include both the internal wave dynamics and the remote forcing from the tropical eastern Pacific SST anomaly. The remote forcing from the tropical eastern Pacific SST anomaly is particularly of importance to the changes of NPO pattern, since the patterns of NPO become similar to each other for the two subperiods if the variability associated with ENSO is removed from the NPO time series. In the regional period, the tropical eastern Pacific SST anomaly has a dominant influence on the NPO, whereas it is not in the global period. Hence the wave process in the middle and high latitudes becomes important in the latter period. The EP flux associated with the NPO indicates that anomalous stationary waves propagate from the subtropical-central Pacific to the northern Pacific in the regional period, inducing an elongated dipole structure of the NPO in the Pacific sector. However, in the global period, this northward propagation of wave activity shifts to the eastern Pacific. In the meantime, over the extratropics of East Asia there are enhanced northward wave propagations, inducing the center of NPO to be shifted to the west of the dateline.

[24] When we compare our results with those of *Walter and Graf* [2002], it is interesting to notice that the regional period for NPO is roughly corresponding to the global period for the NAO and vice versa. Although *Walter and Graf* [2002] mainly discussed the atmosphere-ocean covariability in JFM and we mainly focus on DJF, it seems to be conceivable that the NAO has a significant influence on hemispheric circulation in the middle and high latitudes when the influence of NPO is very local, and vice versa. From our results alone, we cannot determine the physical mechanism leading to this kind of transition. Therefore further researches are needed in the future, especially by using coupled atmosphere-ocean model.

[25] **Acknowledgments.** We thank the three reviewers for their helpful comments and suggestions. This work is supported by the Chinese Key Developing Program for Basic Sciences (grant 2004CB418303) and the National Natural Science Foundation of China (grants 40375021 and 40523001).

## References

Allan, R. J., and T. J. Ansell (2006), A new globally complete monthly historical gridded mean sea level pressure dataset (HadSLP2): 1850–2004, *J. Clim.*, *19*, 5816–5842.

Andrews, D. G., J. R. Holton, and C. B. Leovy (1987), *Middle Atmosphere Dynamics*, 489 p., Elsevier, New York.

Bjerknes, J. (1964), Atlantic air-sea interaction, *Adv. Geophys.*, *10*, 1–82.

Chen, W., M. Takahashi, and H.-F. Graf (2003), Interannual variations of stationary planetary wave activity in the northern winter troposphere and stratosphere and their relations to NAM and SST, *J. Geophys. Res.*, *108*(D24), 4797, doi:10.1029/2003JD003834.

Deser, C., and M. L. Blackmon (1993), Surface climate variations over the North Atlantic ocean during winter: 1900–1989, *J. Clim.*, *6*, 1743–1753.

Gong, D., S. Wang, and J. Zhu (2001), East Asian winter monsoon and Arctic Oscillation, *Geophys. Res. Lett.*, *28*(10), 2073–2076.

Guo, D., and Z. Sun (2004), Relationships of winter North Pacific Oscillation anomalies with the East Asian Winter Monsoon and the weather and climate in China (in Chinese), *J. Nanjing Inst. Meteorol.*, *27*, 461–470.

Horel, J. D., and J. M. Wallace (1981), Planetary-scale atmospheric phenomena associated with the Southern Oscillation, *Mon. Weather Rev.*, *109*, 813–829.

Hurrell, J. W. (1995), Decadal trends in the North Atlantic Oscillations: Regional temperature and precipitation, *Science*, *269*, 676–679.

Hurrell, J. W. (1996), Influence of variations in the extratropical wintertime teleconnections on Northern Hemisphere temperature, *Geophys. Res. Lett.*, *23*(6), 665–668.

Hurrell, J. W., and H. van Loon (1997), Decadal variations in climate associated with the North Atlantic Oscillation, *Clim. Change*, *36*, 301–326.

Hurrell, J. W., Y. Kushnir, G. Ottersen, and M. Visbeck (2003), *The North Atlantic Oscillation: Climatic Significance and Environmental Impact*, 279 p., Geophys. Monogr. Ser., 134.

Kalnay, E., et al. (1996), The NCEP/NCAR 40-year reanalysis project, *Bull. Am. Meteorol. Soc.*, *77*, 437–472.

Karoly, D. J., R. A. Plumb, and M. Ting (1989), Examples of the horizontal propagation of quasi-stationary waves, *J. Atmos. Sci.*, *46*, 2802–2811.

Kistler, R., et al. (2001), The NCEP-NCAR 50-year reanalysis: Monthly means CD-ROM and documentation, *Bull. Am. Meteorol. Soc.*, *82*, 247–268.

Kushnir, Y. (1994), Interdecadal variations in the North Atlantic sea surface temperature and associated atmospheric conditions, *J. Clim.*, *7*, 141–157.

Kutzbach, J. E. (1970), Large-scale features of the monthly mean Northern Hemisphere anomaly maps of sea level pressure, *Mon. Weather Rev.*, *98*, 708–716.

North, G. R., F. J. Moeng, T. L. Bell, and R. F. Cahalan (1982a), The latitude dependence of the variance of zonally averaged quantities, *Mon. Weather Rev.*, *110*, 319–326.

North, , T. L. Bell, R. F. Cahalan, and F. J. Moeng (1982b), Sampling errors in the estimation of empirical orthogonal functions, *Mon. Weather Rev.*, *110*, 699–706.

Plumb, R. A. (1985), On the three-dimensional propagation of stationary waves, *J. Atmos. Sci.*, *42*, 217–229.

Rayner, N. A., D. E. Parker, E. B. Horton, C. K. Folland, L. V. Alexander, D. P. Rowell, E. C. Kent, and A. Kaplan (2003), Global analyses of sea surface temperature, sea ice, and night marine air temperature since the late nineteenth century, *J. Geophys. Res.*, *108*(D14), 4407, doi:10.1029/2002JD002670.

Rogers, J. C. (1979), The north Pacific oscillation and eigenvectors of Northern Hemisphere atmospheric circulation during winter, *NCAR Coop. Thesis No. 56*, 177 p., *Natl. Cent. for Atmos. Res.*, Boulder, Colo.

Rogers, J. C. (1981), The North Pacific Oscillation, *Int. J. Climatol.*, *1*, 39–57.

Rogers, J. C., and H. van Loon (1979), The seesaw in winter temperature between Greenland and Northern Europe: Part II. Some oceanic and atmospheric effects in middle and high latitudes, *Mon. Weather Rev.*, *107*, 509–519.

Torrence, C., and G. P. Compo (1998), A practical guide to wavelet analysis, *Bull. Am. Meteorol. Soc.*, *79*, 61–78.

Trenberth, K. E., and J. W. Hurrell (1994), Decadal atmosphere-ocean variations in the Pacific, *Clim. Dyn.*, *9*, 303–319.

Uppala, S. M., et al. (2005), The ERA-40 re-analysis, *Q. J. R. Meteorol. Soc.*, *131*, 2961–3012.

van Loon, H., and J. C. Rogers (1978), The seesaw in winter temperature between Greenland and Northern Europe: Part I. General description, *Mon. Weather Rev.*, *106*, 296–310.

Walker, G. T., and E. W. Bliss (1932), World Weather V, *Mem. R. Meteorol. Soc.*, *4*, 53.

Wallace, J. M., and D. S. Gutzler (1981), Teleconnections in the geopotential height field during the northern hemisphere winter, *Mon. Weather Rev.*, *109*, 784–812.

Wallace, J. M. and Q. Jiang (1987), On the observed structure of the interannual variability of the atmosphere-ocean climate system, in *Atmospheric and Oceanic Variability*, edited by H. Cattle, p. 17–43, Royal Meteorology Society, Melbourne.

Wallace, J. M., C. Smith, and Q. Jiang (1990), Spatial patterns of atmosphere-ocean interaction in the northern winter, *J. Clim.*, *3*, 990–998.

Walter, K., and H.-F. Graf (2002), On the changing nature of the regional connection between the North Atlantic Oscillation and sea surface temperature, *J. Geophys. Res.*, *107*(D17), 4338, doi:10.1029/2001JD000850.

Wu, R. G., J. L. Kinter III, and B. P. Kirtman (2005), Discrepancy of interdecadal changes in the Asian region among the NCEP-NCAR reanalysis, objective analyses, and observations, *J. Clim.*, *18*, 3048–3067.

Yang, S., and W. J. Gutowski (1994), GCM simulations of the three-dimensional propagation of stationary waves, *J. Clim.*, *7*, 414–433.

Yang, S., K.-M. Lau, and K.-M. Kim (2002), Variations of the East Asian Jet Stream and Asian-Pacific-American Winter Climate Anomalies, *J. Clim.*, *15*, 306–325.

W. Chen and R. Huang, Center for Monsoon System Research, Institute of Atmospheric Physics, Chinese Academy of Sciences, Beijing, 100080, China. (cw@post.iap.ac.cn)

L. Wang, Graduate University of Chinese Academy of Sciences, Beijing, 100049, China.